AD_____

Award Number: DAMD17-00-1-0274

TITLE: Structure-Based Design of erbB-2 Selective Small Molecule Kinase Inhibitors

PRINCIPAL INVESTIGATOR: Shaomeng Wang, Ph.D.

CONTRACTING ORGANIZATION: Georgetown University Medical Center
Washington, DC 20057

REPORT DATE: July 2001

TYPE OF REPORT: Annual

PREPARED FOR: U.S. Army Medical Research and Materiel Command
Fort Detrick, Maryland 21702-5012

REPORT DOCUMENTATION PAGE

Form Approved
OMB No. 074-0188

1. AGENCY USE ONLY (Leave blank)	2. REPORT DATE	3. REPORT TYPE AND DATES COVERED
	July 2001	Annual (1 Jul 00 - 30 Jun 01)

4. TITLE AND SUBTITLE
Structure-Based Design of erbB-2 Selective Small Molecule Kinase Inhibitors

5. FUNDING NUMBERS
DAMD17-00-1-0274

6. AUTHOR(S)
Shaomeng Wang, Ph.D.

7. PERFORMING ORGANIZATION NAME(S) AND ADDRESS(ES)
Georgetown University Medical Center
Washington, DC 20057

E-Mail: shaomeng@umich.edu

8. PERFORMING ORGANIZATION REPORT NUMBER

9. SPONSORING / MONITORING AGENCY NAME(S) AND ADDRESS(ES)
U.S. Army Medical Research and Materiel Command
Fort Detrick, Maryland 21702-5012

10. SPONSORING / MONITORING AGENCY REPORT NUMBER

11. SUPPLEMENTARY NOTES

12a. DISTRIBUTION / AVAILABILITY STATEMENT
Approved for Public Release; Distribution Unlimited

12b. DISTRIBUTION CODE

13. ABSTRACT ***(Maximum 200 Words)***

14. SUBJECT TERMS
Breast Cancer

15. NUMBER OF PAGES
14

16. PRICE CODE

17. SECURITY CLASSIFICATION OF REPORT	18. SECURITY CLASSIFICATION OF THIS PAGE	19. SECURITY CLASSIFICATION OF ABSTRACT	20. LIMITATION OF ABSTRACT
Unclassified	Unclassified	Unclassified	Unlimited

Table of Contents

Task 1. **Molecular modeling, Structure-based database searching, and computational docking** (1-24 months)

- **1.a. Further refinement of the erbB-2 and EGFR models** (1-6 months).

Experimental 3D structure (including the kinase domain) of either erbB-2 or EGFR has not been determined. Fortunately, the structures of the kinase domain of a number of receptor tyrosine kinases have been determined through X-ray crystallography with high resolutions. Protein kinases, including erbB-2 and EGFR, have an active and inactive conformation. Analysis of the X-ray structures of several kinases, including insulin receptor kinase and FGFR kinase showed that when an ATP analog or a small molecule kinase inhibitor bound to the ATP binding site of the kinase domain, the kinase always assumes an active conformation. Accordingly, it is hypothesized that erbB-2 and EGFR also assume an active conformation when bound to an inhibitor.

We have used three template protein structures all with high resolution to model the active conformations of erbB-2 and EGFR. The first is the structure of the kinase domain of the insulin receptor kinase bound to an ATP analog and a peptide substrate, which was determined with X-ray crystallography to an accuracy of 1.9 Å (PDB code: 1IR3). The second is the structures of the kinase domain of the human FGFR1, either alone or in the complex with a small molecule kinase inhibitor SU4984, or SU5402, or PD173074, whose structures were determined with X-ray crystallography to an accuracy of from 2.0 to 2.5 Å (PDB codes: 1FGK, 1AGW, 1FGI and 2FGI). The third is the structure of the human tyrosine protein C (SRC), whose structure was determined with X-ray crystallography to an accuracy of 1.5 Å (PDB code: 1FMK). These proteins share the highest degree of homology with erbB-2 and EGFR in their kinase domains among all the structures in the Protein Databank (PDB). The rational of using structures of three different kinase domains for homology modeling is to investigate if significant differences were found with modeled structures when different template structures were used. The sequence alignment between the kinase domains of erbB-2 and EGFR and these template proteins is shown in Figure 1.

Based upon the sequence alignment, erbB-2 and the insulin receptor kinase domains have an amino acid identity of 35% and a similarity of 52%; erbB-2 and the FGFR1 and kinase domains have an amino acid identity of 37% and a similarity of 55%; erbB-2 and the SRC kinase domains have an amino acid identity of 41% and a similarity of 55%. There is 10% of amino acid gap (insertion and deletion) between erbB-2 and the insulin receptor kinase domains, 8% gap between erbB-2 and the FGFR1 and kinase domains and 5% gap between erbB-2 and the SRC kinase domains. Accurate modeling of these gap regions is a major challenge and problem in homology modeling at the present time. Fortunately, the major gap is located in a loop region

connecting two helices in all the three template proteins, which is approximately 20 Å away from the ATP/inhibitor binding site. Therefore, the potential problem with accurate modeling the gap region is of minimal significance in our structure-based design erbB-2 kinase inhibitors. It is of note that even in the X-ray structures of insulin receptor, SRC and FGRF1, the coordinates of the loop region residues were missing, due to the high flexibility of the loop region.

Figure 1. Sequence alignment between erbB-2, EGFR, Insulin receptor kinase, FGFR1, and SRC tyrosine kinase and this alignment was used for homology modeling. The residues that form the ATP binding pocket are highlighted.

```
VKVLGSGAFGTVYKG-IWIPDGENVKIPVAIKVLRENTSPKANKEILDEAYVMAGVGSP-YVSRLLGI (erbB2)
IKVLGSGAFGTVYKG-LWIPEGEKVKIPVAIKELREATSPKANKEILDEAYVMASVDNP-HVCRLLGI (EGFR)
GKPLGEGAFGQVVLA-EAIGLPNRVT-KVAVKMLKSDATEKDLSDLISEMEMMKMIGKHKNIINLLGA (1IR3)
LRELGQGSFGMVYEGNARDIIKGEAETRVAVKTVNESASLRERIEFLNEASVMKGFTCH-HVVRLLGV (1FGK)
EVKLGQGCFGEVWMGTW------NGTTRVAIKTLKPGTMSPE--AFLQEAQVMKKL-RHEKLVQLYAV (1FMK)

                    (Helix region) (loop region)

CL-TSTVQLVTQLMPYGCLLDHVRENRGRLGSQD--------LLNWCM-QIAKGMSYLEDVRLVHRDLA
CL-TSTVQLITQLMPFGCLLDYVREHKDNIGSQY--------LLNWCV-QIAKGMNYLEDRRLVHRDLA
CTQDGPLYVIVEYASKGNLREYLQARR-QLSSKD--------LVS-CAYQVARGMEYLASKKCIHRDLA
VSKGQPTLVVMELMAHGDLKSYLRSLRPEAENNPGRPPPTLQEMIQMAAEIADGMAYLNAKKFVHRDLA
-VSEEPIYIVTEYMSKGSLLDFLKGETGK--------YLRLPQLVDMAAQIASGMAYVERMNYVHRDLR

ARNVLVKSPNHVKITDFGLARLLDIDETEYHADGGKVPIKWMALESILRRRFTHQSDVWSYGVTVWELM...
ARNVLVKTPQHVKITDFGLAKLLGAEEKEYHAEGGKVPIKWMALESILHRIYTHQSDVWSYGVTVWELM...
ARNVLVTEDNVMKIADFGLA--------DYYKKG-RLPVKWMAPEALFDRIYTHQSDVWSFGVLLWEIF...
ARNCMVAHDFTVKIGDFGMTRDIETDRKG---GKGLLPVRWMAPESLKDGVFTTSSDMWSFGVVLWEIT...
AANILVGENLVCKVADFGLAR---------------FPIKWTAPEAALYGRFTIKSDVWSFGILLTELT...
```

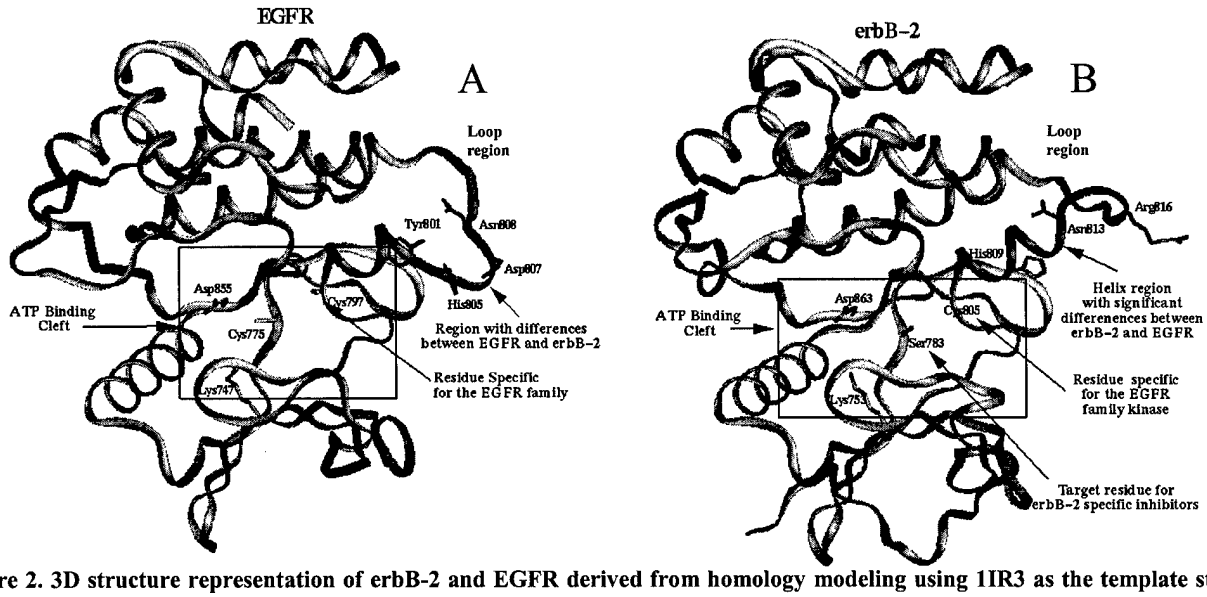

Figure 2. 3D structure representation of erbB-2 and EGFR derived from homology modeling using 1IR3 as the template structure. The crucial differences in residues between erbB-2 EGFR and other kinases in their ATP binding sites are highlighted, including a unique cysteine residue (Cys805 in erbB2 and Cys775 in EGFR) and a number of residues in the helix region.

Many homology modeling studies, including blind structure predictions from the Critical Assessment of Structure Prediction (CASP) experiments, have shown that when the homology between the target and template proteins are more than 30%, an accurate structure of the target protein can be reliably obtained. Therefore, the high degree of homology (35-41% of amino acid identity and 52-55% of amino acid similarity) between erbB-2, or EGFR, and these three different template proteins should allow us to achieve an accurate modeling of the 3D structure of the erbB-2 and EGFR kinase domains.

The sequence alignment between EGFR kinase domain and these three different kinase domains is also provided in Figure 1. The amino acid identity and similarity between EGFR and these three kinase domains are comparable to that between erbB-2 and these three kinase domains. The amino acid identity is 35-38%, the amino acid similarity is 54-55% and the gap is 4-5%. Similar to erbB-2, the gap is located in the region connecting the two helices and 20 Å away from the ATP binding site. Therefore, it is expected that an accurate 3D structure of the EGFR kinase domain can be obtained based upon the X-ray structures of these template proteins using homology modeling approach.

A homology modeling program, MODELLER, developed by Dr. Sali at Rockfellor University has been shown to be able to provide a fairly accurate 3D structure for a target protein when there is at least 30% of sequence homology between the target and the template protein. The predictive ability of MODELLER

program has been validated through a number of unbiased and blind structural prediction tests. Accordingly, MODELLER was chosen to model the 3D structures of the erbB-2 and EGFR kinase domains based upon the sequence alignment shown in Figure 1 and three X-ray structures of insulin receptor kinase (pdb code: 1IR3), FGFR1 kinase domain (pdb code: 1FGI), and SRC tyrosine kinase (pdb code: 1FMK).

With such high degree homology between target proteins and template proteins, it is expected that homology modeling should provide accurate structural information for the main chain of the proteins. However, the side chain conformations may need to be further refined, although MODELLER does use a side chain library to model the side chain conformations. For this purpose, we have carried out extensive molecular dynamics simulations using the CHARMM program. The force field used in the simulations to represent the proteins is the latest CHARMM force field (version 24). To accurately model the solvent environment, TIP3P water model was used to represent the water molecules. It is of note that the CHARMM force field was developed specifically to be compatible with the TIP3P water model for modeling proteins and DNAs. Constant temperature MD simulations were carried out at 300 K for 1000 ps or longer. Since it is believed that the main chain conformations were modeled fairly accurately, constraints were applied to main chain atoms. The refined structures of erbB-2 and EGFR kinase domains using IR3 as the template structure are shown in Figure 2.

It is important and instructive to compare the structures of erbB-2 and EGFR kinase domains with the experimental structures of other kinase domains to gain a fundamental understanding on the structural similarity and difference between these kinases. Such analysis should provide the structural basis for the structure-based design of selective and potent kinase inhibitors.

Based upon our modeled structures, we found that erbB-2 and EGFR have a very similar ATP binding site in terms of general shape as compared to other receptor kinases such as insulin receptor tyrosine kinase. However, among the residues that form the ATP binding site, there exist significant differences between the EGFR family (erbB2 and EGFR) and other kinases. Therefore, it is expected that potent and highly selective inhibitors can be designed against the EGFR family kinase. Indeed, a number of highly potent and selective reversible EGFR family kinase inhibitors have been reported.

It is of note that a cysteine residue (Cys805 in erbB-2 or Cys797 in EGFR), located on one end of a helix immediately outside the ATP binding pocket (Figure 2), is quite unique for EGFR and erbB-2 and is not shared by other receptor kinases. Using this single unique cysteine for the EGFR family, potent and highly selective, irreversible kinase inhibitors for the EGFR family have been successfully designed[6; 12; 16].

Comparison between the modeled structures of erbB-2 and EGFR showed that inside the ATP binding site, the apparent residue difference is Ser783 (Figure 2) in erbB-2, whose corresponding residue is Cys775 in

EGFR. It is of note that a number of residues located on the helix immediately outside the ATP binding pocket differ between erbB-2 and EGFR. For example, His809 in erbB-2 aligns with Tyr801 in EGFR, Asn813 in erbB-2 aligns with His805 in EGFR and Arg116 in erbB-2 aligns with Asn808 in EGFR. The residue differences between erbB-2 and EGFR will be used as our specific targeted residues for the design of erbB-2 selective inhibitors. The apparent residue differences with this helix between EGFR and erbB-2 may also translate into a conformational difference with this helix in terms of both orientation and conformational flexibility. It is of note that the Cys805 in erbB-2 or Cys797 in EGFR is located at the end of this helix, whose conformation will be affected by a conformational change in the helix. A key element is our proposal is to explore these structural differences between erbB-2, EGFR and other kinases for inhibitor design to achieve high specificity.

- **1.b. Performance of structure-based database searching on both the ACD and NCI 3D-database to identify potential kinase inhibitors.**(1-24 months).

In the last few years, we have built four large 3D-databases of small molecules, which consist of more than 650,000 organic synthetic compounds and natural products. These large 3D-databases are valuable resources for drug design and have been used successfully in several projects for novel lead discovery. To date, we have completed the structure-based search of the National Cancer Institute's 3D-database of 225,00 structurally diverse synthetic compounds and natural products to identify potential erbB-2 kinase inhibitors using the modeled erbB-2 structure. First we used the DOCK[22] program developed by Dr. Kuntz at the UCSF to determine whether compounds can fit into the ATP binding site of erbB-2 in terms of their shape. For the top 10,000 compounds that satisfy the shape criterion, we used the program MCDOCK[23] developed in our laboratory to further evaluate which potential inhibitors most effectively interact with erbB-2 kinase domain binding site using van der Waals and electrostatic interaction energy and taken account the conformational flexibility of these potential inhibitors. To avoid selecting highly charged molecules, the electrostatic interaction energy was scaled by a factor of 10. The top 2000 compounds with most favorable interaction energy identified through the MCDOCK calculations were further examined to identify compounds with low molecular weight (<800), simple chemical structures. About 500 compounds met such criteria. Of which, we selected 200 compounds with sufficiently structural diversity as potential erbB-2 kinase inhibitors for biological screening, as detailed below.

Task 2. Biological Confirmation of Potential Kinase Inhibitors (**1-24 months**)

2.a. Initial cell based screening for activity and specificity.

First, we used the human breast cancer cell line MDA-453 that overexpresses erbB-2 resulted from gene amplification to screen these potential erbB-2 kinase inhibitors for their ability to inhibit erbB-2 auto

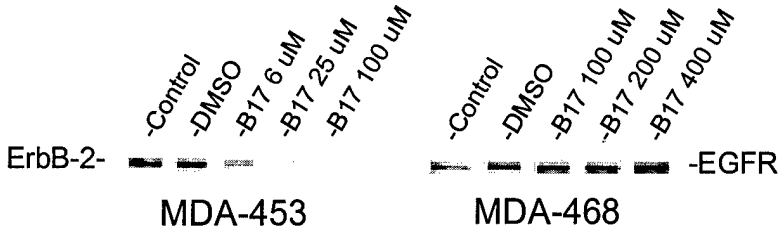

Figure 3. MDA-453 and MDA-468 cells were grown in 12-well plates to 90% confluence and then changed into serum-free medium overnight. Cells were treated with B17 for 30 min and extracts were made for western blotting with anti-phosphortyrosine mAb.

phosphorylation. 11 out of 200 compounds inhibited more than 90% of erbB-2 phosphorylation at 100 μM. We then carried out a dose-dependent phosphorylation assay in MDA-453 cell line that overexpresses erbB-2 and MDA-468 cell line that overexpresses the EGFR to test both the potency and selectivity. Of which, **seven**

Char I. Chemucal Structures of novel erbB-2 small molecule inhibitors discovered from structure-based 3D-database searching.

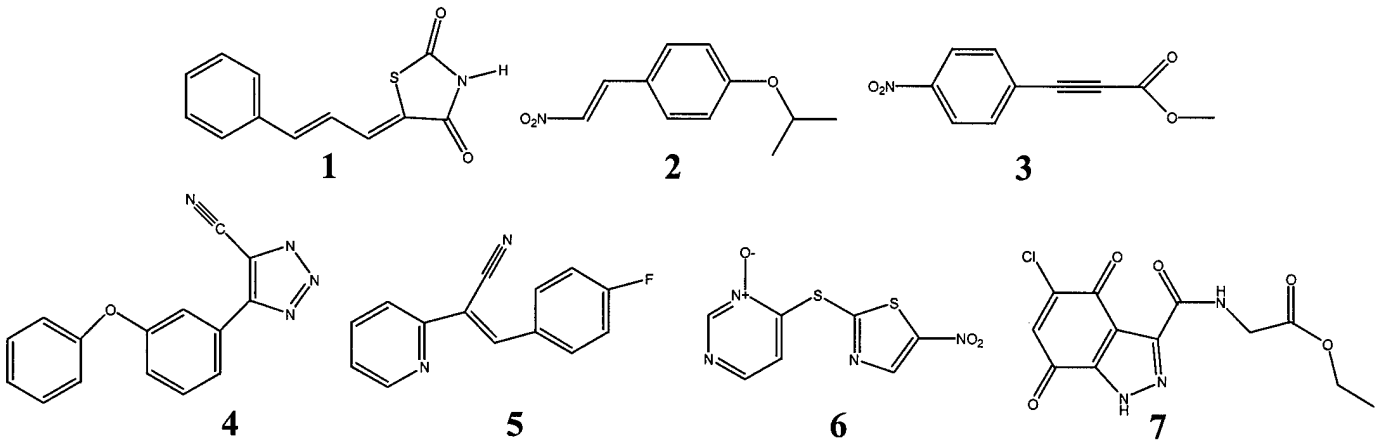

compounds were found to have relative selectivity in inhibiting erbB-2 phosphorylation in MDA-453 cells *versus* in inhibiting EGFR auto-phosphorylation the MDA-468 cells. The chemical structures of these lead compounds are shown in Chart I. And their activity are summarized in **Table 1**.

As can be seen from Table 1, these compounds have an IC50 from 2.5 to 50 μM in cell-based inhibition erbB-2 phosphorylation. The most potent compound **3** (**B17**) has an IC_{50} value of 2.5 μM, and importantly, **B17** showed a selectivity more than 160-fold between its potencies in inhibition of erbB-2 and EGFR auto-phosphorylation (**Fig. 3**). In addition to **B17**, a number of these compounds may be considered as novel leads. Compound **2** has an IC_{50} of 5 μM and a selectivity between erbB-2 and EGFR over 80-fold. Compounds **4** and **5** both have an IC_{50} value of 25 μM in inhibition of erbB-2 auto-phosphorylation and **5** also showed more than 8-fold selectivity between erbB-2 and EGFR. Molecular modeling studies showed that specific modifications with these compounds can be made to dramatically improve their potency. These compounds represent new classes kinase inhibitors with novel chemical scaffolds. Furthermore, **2** and **3** (**B17**) display approximately 100-fold selectivity between erbB-2 and EGFR. Therefore, a number of these compounds may be considered as attractive leads for further optimization to improve their potency and selectivity. Since **3** (**B17**) is the most potent lead among these compounds, we have carried further characterization on **3** (**B17**), as detailed below.

Table 1. Summary of the cell-based inhibitory activity of seven novel lead compounds.

	1	**2**	**3 (B17)**	**4**	**5**	**6**	**7**
MDA-453, IC_{50}, uM	50	5	**2.5**	25	25	25	15
MDA-468, IC_{50}, uM	>100	>400	**>400**	400	>400	>400	>400
Selectivity EGFR v.s. erbB-2	>2	>80	**>160**	8	>8	>8	>27
Inhibitor Type	R*	I**	**I**	R	R	R	I

*R: reversible inhibitor; **I: irreversible inhibitor

2.b. Inhibition of ligand-induced phosphorylation and further testing of specificity using model cell lines.

To further assess that the potency and selectivity of **B17**, we utilized several model cell lines. The NIH-3T3 cells were transfected with either EGFR, erbB-2 or the chimeric EGFR (extracellular) and erbB-2 (intracellular) receptor. The chimeric EGFR (extracellular) and erbB-2 (intracellular) receptor has an EGF ligand binding site in its extracellular domain but has an intracellular erbB-2 kinase domain. Thus, although both EGFR and chimeric EGFR/erbB-2 depend on addition of EGF to induce phosphorylation, they have different kinase domains. Overexpression of erbB-2 receptor resulted in a high level of auto-phosphoyrlation in these cells. A more erbB-2 specific kinase inhibitor, such as **B17** should inhibit the EGF induced

phosphorylation in the NIH 3T3 cells transfected with the chimeric EGFR/erbB-2 receptor but should be much less active in inhibiting the phosphorylation induced by EGF in the NIH 3T3 cell line transfected with EGFR. Moreover, it was also predicted that **B17** should also inhibit the auto-phosphorylation activity in the NIH 3T3 cell line overexpressed erbB-2. As shown in **Fig. 4**, **B17** selectively inhibits the EGF-induced erbB-2 kinase activity in the NIH 3T3 cells transfected with the chimeric EGFR/erbB-2 receptor with an IC_{50} value of 1.3 μM, but did not show appreciable inhibition of the EGFR kinase activity in 3T3-EGFR cells with concentrations up to 100 μM. **B17** also inhibits the auto-phosphorylation of erbB-2 in the NIH 3T3/erbB-2 cells with same potency. Thus, we showed that **B17** is a potent and selective erbB-2 specific kinase inhibitor, with an selectivity approximately 100-fold between erbB-2 and its closely related family member EGFR using model cell lines with same genetic backgrounds.

To further assess its selectivity, we have tested **B17** against insulin receptor or insulin-like growth factor receptor I kinase (NWT21) in 3T3 transfected cells, and PDGF (BB) receptor in wild-type 3T3 cells treated

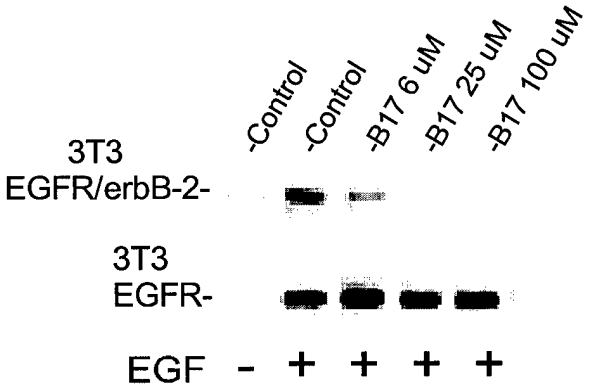

Figure 4. Inhibition of the ligand-induced phosphorylation by B17 in NIH3T3 cells transfected with either wild-type EGFR or chimeric EGFR/erbB-2 recptor kinase. Cells were treated same as in Fig. 3, but with addition of EGF at 10nM for 5 min.

with PDGF (BB). We also used endothelial cell line HUVEC to test the effect of **B17** on VEGF receptor kinase and FGF receptor after treated with VEGF or bFGF, respectively. In all these tests, no appreciable inhibition was observed with **B17** against these kinases (data not shown).

c.5.f. Inhibition of cell proliferation and selectivity.

We further tested the ability of **B17** in inhibition of cell growth using a number of cell lines overexpressed either erbB-2 or EGFR, or neither. Among a number of cell lines we used, MDA-453 overexpresses erbB2, while MDA-468 overexpresses EGFR and MDA-231 overexpresses neither. **B17** had an IC_{50} value of 0.3 μM in MDA-453. In MDA-468, **B17** had 25% of inhibition at 5 μM (IC50 >5 μM). Thus, **B17**

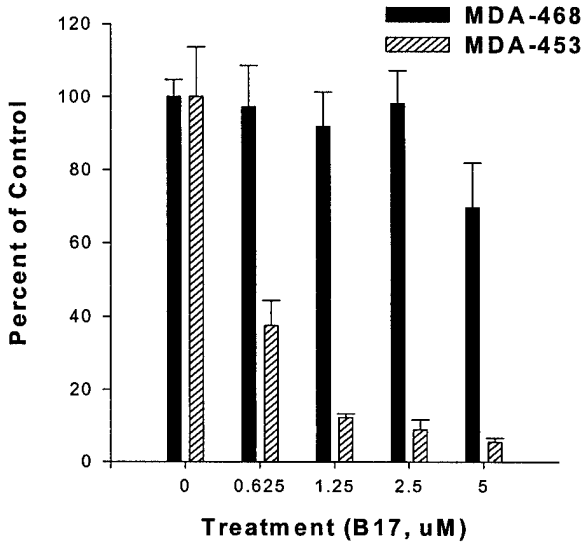

Figure 5. Inhibition of cell proliferation by B17 in MDA-453 and MDA-468 cells.

displays a relative selectivity of more than 15-fold between cell lines overexpressed erbB-2 and EGFR. In control cell line MDA-231, **B17** also has an estimated IC_{50} value more than 5 μM, 15-times less potent than its activity in MDA-453 overexpressed erbB-2.

2.c. Inhibition of erbB-2 and EGFR mediated MAP kinase activity.

ErbB-2 and EGFR mediate the down-stream MAP kinase activity. It was thus predicted that a more selective kinase inhibitor such as **B17** should significantly inhibit the erbB-2 mediated MAP kinase activity in MDA-453 but not the EGFR mediated MAP kinase activity in MDA-468. Indeed, our results showed that the MAP kinase activity in MDA-453 was inhibited by **B17** with a potency similar to that in inhibition of erbB-2 auto-phosphorylation, while the MAP kinase activity in MDA-468 was not inhibited with concentration up to

400 μM. These results indicated that **B17** specifically inhibits the erbB-2 mediated but not EGFR mediated MAP kinase signaling pathway in cells.

2.d. *In vivo* Modulation of erbB-2 phosphorylation and MAP kinase activity.

To investigate the *in vivo* effect of **B17** in modulation of erbB-2 or EGFR phosphorylation under systemic administration in animals, we have utilized BT-474/M1 or A431 xenografts model (BT-474/M1 was kindly provided by Dr. C. Benz, UCSF) which formed progressive tumors in nude mice. We first treated mice bearing BT-474/M1 or A431 tumor intraperitoneally (i.p) with **B17** at 100 mg/kg. We excised tumors at 24 hours after treatment, then prepared homogenates of the tumors and determined levels of phosphorylated erbB-2 or EGFR by western blotting analysis. Treatment with **B17** almost completely suppressed erbB-2 phosphorylation and MAP kinase activation (**Figure 6**), while having no appreciable inhibition of on EGFR phosphorylation in A431 cells (data not shown). It is of note that **B17** had no effects on total erbB-2 protein, suggesting that its inhibition in erbB-2 kinase activity is not due to inhibition of erbB-2 expression or enhancing protein degradation.

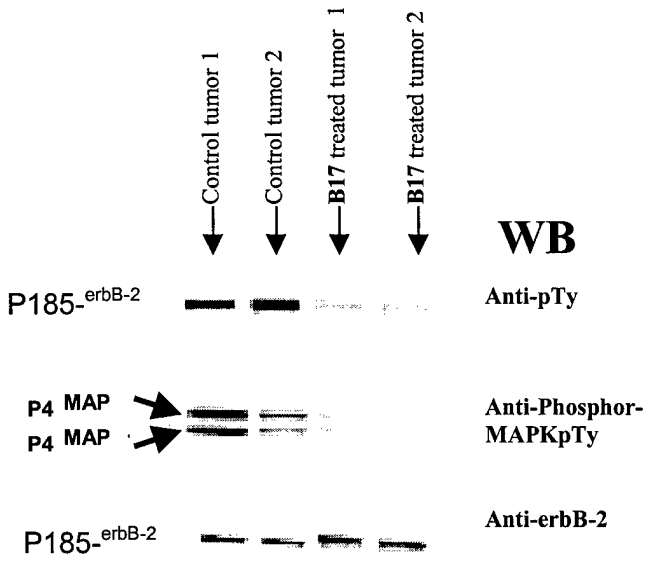

Figure 6. ***In Vivo* Effects of** B17 **on Phosphorylation of erbB-2, MAP kinase and total erbB-2 in BT-474/M1 Cells (24 Hours after Intraperitonia Treatment)**

Project Plan for Year 2.

- One major objective of this project is year 2 (13-24 months) aims at further improvement of the potency of the lead compounds. Toward this end, we will focus on the optimization of the most potent lead compound **B-17 (Task 1c and 1d)**.

- The second major objective of this project in year 2 (13-24) is to test the anticancer activity of B-17 and its more potent analogues using human breast cancer xenograft models in nude mice. **(Task 3)**.

- The third major goal of this project is to prepare scientific publications for the very exciting results we have obtained to date on this project.